

¹ **Critical transitions and the fragmenting of global forests**

² **Leonardo A. Saravia^{1 3}, Santiago R. Doyle¹, Benjamin Bond-Lamberty²**

³ 1. Instituto de Ciencias, Universidad Nacional de General Sarmiento, J.M. Gutierrez 1159 (1613), Los
⁴ Polvorines, Buenos Aires, Argentina.

⁵ 2. Pacific Northwest National Laboratory, Joint Global Change Research Institute at the University of
⁶ Maryland–College Park, 5825 University Research Court #3500, College Park, MD 20740, USA

⁷ 3. Corresponding author e-mail: lsaravia@ungs.edu.ar

⁸ **keywords:** Forest fragmentation, early warning signals, percolation, power-laws, MODIS, critical transitions

⁹ **Running title:** Critical fragmentation in global forest

¹⁰ **Abstract**

¹¹ 1. Forests provide critical habitat for many species, essential ecosystem services, and are coupled to
¹² atmospheric dynamics through exchanges of energy, water and gases. One of the most important
¹³ changes produced in the biosphere is the replacement of forest areas with human dominated landscapes.
¹⁴ This usually leads to fragmentation, altering the sizes of patches, the structure and function of the
¹⁵ forest. Here we studied the distribution and dynamics of forest patch sizes at a global level, examining
¹⁶ signals of a critical transition from an unfragmented to a fragmented state.

¹⁷ 2. We used MODIS vegetation continuous field to estimate the forest patches at a global level and de-
¹⁸ fined wide regions of connected forest across continents and big islands. We search for critical phase
¹⁹ transitions, where the system state of the forest changes suddenly at a critical point in time; this
²⁰ implies an abrupt change in connectivity that causes an increased fragmentation level. We studied the
²¹ distribution of forest patch sizes and the dynamics of the largest patch over the last fourteen years,
²² as the conditions that indicate that a region is near a critical fragmentation threshold are related to
²³ patch size distribution and temporal fluctuations of the largest patch.

²⁴ 3. We found some evidence that allows us to analyze fragmentation as a critical transition: most regions
²⁵ followed a power-law distribution over the 14 years. We also found that the Philippines region probably
²⁶ went through a critical transition from a fragmented to an unfragmented state. Only the tropical forest
²⁷ of Africa and South America met the criteria to be near a critical fragmentation threshold.

28 4. This implies that human pressures and climate forcings might trigger undesired effects of fragmentation,
29 such as species loss and degradation of ecosystems services, in these regions. The simple criteria
30 proposed here could be used as an early warning to estimate the distance to a fragmentation threshold
31 in forest around the globe and a predictor of a planetary tipping point.

32 Introduction

33 Forests are one of the most important biomes on earth, providing habitat for a large proportion of species
34 and contributing extensively to global biodiversity (Crowther et al., 2015). In the previous century human
35 activities have influenced global bio-geochemical cycles (Bonan, 2008; Canfield, Glazer, & Falkowski, 2010),
36 with one of the most dramatic changes being the replacement of 40% of Earth's formerly biodiverse land
37 areas with landscapes that contain only a few species of crop plants, domestic animals and humans (J. A.
38 Foley et al., 2011). These local changes have accumulated over time and now constitute a global forcing
39 (Barnosky et al., 2012).

40 Another global scale forcing that is tied to habitat destruction is fragmentation, which is defined as the
41 division of a continuous habitat into separated portions that are smaller and more isolated. Fragmentation
42 produces multiple interwoven effects: reductions of biodiversity between 13% and 75%, decreasing forest
43 biomass, and changes in nutrient cycling (Haddad et al., 2015). The effects of fragmentation are not only
44 important from an ecological point of view but also that of human activities, as ecosystem services are deeply
45 influenced by the level of landscape fragmentation (Mitchell et al., 2015).

46 Ecosystems have complex interactions between species and present feedbacks at different levels of organiza-
47 tion (Gilman, Urban, Tewksbury, Gilchrist, & Holt, 2010), and external forcings can produce abrupt changes
48 from one state to another, called critical transitions (Scheffer et al., 2009). These abrupt state shifts cannot
49 be linearly forecasted from past changes, and are thus difficult to predict and manage (Scheffer et al., 2009).
50 Such 'critical' transitions have been detected mostly at local scales (S. R. Carpenter et al., 2011; Drake &
51 Griffen, 2010), but the accumulation of changes in local communities that overlap geographically can prop-
52 agate and theoretically cause an abrupt change of the entire system at larger scales (Barnosky et al., 2012).
53 Coupled with the existence of global scale forcings, this implies the possibility that a critical transition could
54 occur at a global scale (C. Folke et al., 2011; Rockstrom et al., 2009).

55 Complex systems can experience two general classes of critical transitions (R V Solé, 2011). In so-called first
56 order transitions, a catastrophic regime shift that is mostly irreversible occurs because of the existence of
57 alternative stable states (Scheffer et al., 2001). This class of transitions is suspected to be present in a variety
58 of ecosystems such as lakes, woodlands, coral reefs (Scheffer et al., 2001), semi-arid grasslands (Brandon T.
59 Bestelmeyer et al., 2011), and fish populations (Vasilakopoulos & Marshall, 2015). They can be the result of
60 positive feedback mechanisms (Villa Martín, Bonachela, Levin, & Muñoz, 2015); for example, fires in some
61 forest ecosystems were more likely to occur in previously burned areas than in unburned places (Kitzberger,
62 Aráoz, Gowda, Mermoz, & Morales, 2012).

63 The other class of critical transitions are continuous or second order transitions (Ricard V. Solé & Bascompte,
64 2006). In these cases, there is a narrow region where the system suddenly changes from one domain to another,
65 with the change being continuous and in theory reversible. This kind of transitions were suggested to be
66 present in tropical forest (S. Pueyo et al., 2010), semi-arid mountain ecosystems (McKenzie & Kennedy,
67 2012), tundra shrublands (Naito & Cairns, 2015). The transition happens at a critical point where we can
68 observe a distinctive spatial pattern: scale invariant fractal structures characterized by power law patch
69 distributions (Stauffer & Aharony, 1994).

70 There are several processes that can convert a catastrophic transition to a second order transitions (Villa
71 Martín et al., 2015). These include stochasticity, such as demographic fluctuations, spatial heterogeneities,
72 and/or dispersal limitation. All these components are present in forest around the globe (Filotas et al.,
73 2014; Fung, O'Dwyer, Rahman, Fletcher, & Chisholm, 2016; Seidler & Plotkin, 2006), and thus continuous
74 transitions might be more probable than catastrophic transitions. Moreover there is some evidence of recovery
75 in some systems that supposedly suffered an irreversible transition produced by overgrazing (Brandon T
76 Bestelmeyer, Duniway, James, Burkett, & Havstad, 2013; J. Y. Zhang, Wang, Zhao, Xie, & Zhang, 2005)
77 and desertification (Allington & Valone, 2010).

78 The spatial phenomena observed in continuous critical transitions deal with connectivity, a fundamental
79 property of general systems and ecosystems from forests (Ochoa-Quintero, Gardner, Rosa, de Barros Ferraz,
80 & Sutherland, 2015) to marine ecosystems (Leibold & Norberg, 2004) and the whole biosphere (Lenton &
81 Williams, 2013). When a system goes from a fragmented to a connected state we say that it percolates (R
82 V Solé, 2011). Percolation implies that there is a path of connections that involves the whole system. Thus
83 we can characterize two domains or phases: one dominated by short-range interactions where information
84 cannot spread, and another in which long range interactions are possible and information can spread over
85 the whole area. (The term “information” is used in a broad sense and can represent species dispersal or
86 movement.)

87 Thus, there is a critical “percolation threshold” between the two phases, and the system could be driven close
88 to or beyond this point by an external force; climate change and deforestation are the main forces that could
89 be the drivers of such a phase change in contemporary forests (Bonan, 2008; Haddad et al., 2015). There
90 are several applications of this concept in ecology: species' dispersal strategies are influenced by percolation
91 thresholds in three-dimensional forest structure (Ricard V Solé, Bartumeus, & Gamarra, 2005), and it has
92 been shown that species distributions also have percolation thresholds (He & Hubbell, 2003). This implies
93 that pushing the system below the percolation threshold could produce a biodiversity collapse (J. Bascompte
94 & Solé, 1996; Pardini, Bueno, Gardner, Prado, & Metzger, 2010; Ricard V. Solé, Alonso, & Saldaña, 2004);

95 conversely, being in a connected state (above the threshold) could accelerate the invasion of forest into prairie
96 (Loehle, Li, & Sundell, 1996; Naito & Cairns, 2015).

97 One of the main challenges with systems that can experience critical transitions—of any kind—is that the
98 value of the critical threshold is not known in advance. In addition, because near the critical point a small
99 change can precipitate a state shift of the system, they are difficult to predict. Several methods have been
100 developed to detect if a system is close to the critical point, e.g. a deceleration in recovery from perturbations,
101 or an increase in variance in the spatial or temporal pattern (Boettiger & Hastings, 2012; S. R. Carpenter
102 et al., 2011; Dai, Vorselen, Korolev, & Gore, 2012; Hastings & Wysham, 2010).

103 The existence of a critical transition between two states has been established for forest at global scale in
104 different works (Hirota, Holmgren, Nes, & Scheffer (2011); Verbesselt et al. (2016); Staal, Dekker, Xu, &
105 Nes (2016); Wuyts, Champneys, & House (2017)). It was not probed, but is generally believed, that this
106 constitutes a first order catastrophic transition. The regions where forest can grow are not distributed
107 homogeneously, there are demographic fluctuations in forest growth and disturbances produced by human
108 activities. Due to new theoretical advances (Villa Martín, Bonachela, & Muñoz, 2014; Villa Martín et al.,
109 2015) all these factors imply that if these were first order transitions they will be converted or observed as
110 second order continuous transitions. From this basis we applied indices derived from second order transitions
111 to global forest cover dynamics.

112 In this study, our objective is to look for evidence that forests around the globe are near continuous critical
113 point that represent a fragmentation threshold. We use the framework of percolation to first evaluate if
114 forest patch distribution at a continental scale is described by a power law distribution and then examine
115 the fluctuations of the largest patch. The advantage of using data at a continental scale is that for very
116 large systems the transitions are very sharp (R V Solé, 2011) and thus much easier to detect than at smaller
117 scales, where noise can mask the signals of the transition.

118 Methods

119 Study areas definition

120 We analyzed mainland forests at a continental scale, covering the whole globe, by delimiting land areas with
121 a near-contiguous forest cover, separated with each other by large non-forested areas. Using this criterion,
122 we delimited the following forest regions. In America, three regions were defined: South America temperate
123 forest (SAT), subtropical and tropical forest up to Mexico (SAST), and USA and Canada forest (NA). Europe

and North Asia were treated as one region (EUAS). The rest of the delimited regions were South-east Asia (SEAS), Africa (AF), and Australia (OC). We also included in the analysis islands larger than 10^5 km^2 . The mainland region has the number 1 e.g. OC1, and the nearby islands have consecutive numeration (Appendix S4, figure S1-S6). We applied this criterion to delimit regions because we based our study on percolation theory that assumes some kind of connectivity in the study area (see below). Forest ### patch distribution

We studied forest patch distribution in each defined area from 2000 to 2015 using the MODerate-resolution Imaging Spectroradiometer (MODIS) Vegetation Continuous Fields (VCF) Tree Cover dataset version 051 (C. DiMiceli et al., 2015). This dataset is produced at a global level with a 231-m resolution, from 2000 onwards on an annual basis. There are several definition of forest based on percent tree cover (J. O. Sexton et al., 2015); we choose a range from 20% to 30% threshold in 5% increments to convert the percentage tree cover to a binary image of forest and non-forest pixels. This range is centered in the definition used by the United Nations' International Geosphere-Biosphere Programme (Belward, 1996), and studies of global fragmentation (Haddad et al., 2015) and includes the range used in other studies of critical transitions (Xu et al., 2016). Using this range we try to avoid the errors produced by low discrimination of MODIS VCF between forest and dense herbaceous vegetation at low forest cover and the saturation of MODIS VCF in dense forests (J. O. Sexton et al., 2013). We repeat all the analysis for this set of thresholds, except in some specific cases described below. Patches of contiguous forest were determined in the binary image by grouping connected forest pixels using a neighborhood of 8 forest units (Moore neighborhood). The MODIS VCF product defines the percentage of tree cover by pixel, but does not discriminate the type of trees so besides natural forest it includes plantations of tree crops like rubber, oil palm, and forestry land uses [].

Percolation theory

A more in-depth introduction to percolation theory can be found elsewhere (Stauffer & Aharony, 1994) and a review from an ecological point of view is available (B. Oborny, Szabó, & Meszéna, 2007). Here, to explain the basic elements of percolation theory we formulate a simple model: we represent our area of interest by a square lattice and each site of the lattice can be occupied—e.g. by forest—with a probability p . The lattice will be more occupied when p is greater, but the sites are randomly distributed. We are interested in the connection between sites, so we define a neighborhood as the eight adjacent sites surrounding any particular site. The sites that are neighbors of other occupied sites define a patch. When there is a patch that connects the lattice from opposite sides, it is said that the system percolates. When p is increased from low values, a percolating patch suddenly appears at some value of p called the critical point p_c .

154 Thus percolation is characterized by two well defined phases: the unconnected phase when $p < p_c$ (called
155 subcritical in physics), in which species cannot travel far inside the forest, as it is fragmented; in a general
156 sense, information cannot spread. The second is the connected phase when $p > p_c$ (supercritical), species
157 can move inside a forest patch from side to side of the area (lattice), i.e. information can spread over the
158 whole area. Near the critical point several scaling laws arise: the structure of the patch that spans the area
159 is fractal, the size distribution of the patches is power-law, and other quantities also follow power-law scaling
160 (Stauffer & Aharony, 1994).

161 The value of the critical point p_c depends on the geometry of the lattice and on the definition of the
162 neighborhood, but other power-law exponents only depend on the lattice dimension. Close to the critical
163 point, the distribution of patch sizes is:

164 (1) $n_s(p_c) \propto s^{-\alpha}$

165 where $n_s(p)$ is the number of patches of size s . The exponent α does not depend on the details of the
166 model and it is called universal (Stauffer & Aharony, 1994). These scaling laws can be applied for landscape
167 structures that are approximately random, or at least only correlated over short distances (Gastner, Oborny,
168 Zimmermann, & Pruessner, 2009). In physics this is called “isotropic percolation universality class”, and
169 corresponds to an exponent $\alpha = 2.05495$. If we observe that the patch size distribution has another exponent
170 it will not belong to this universality class and some other mechanism should be invoked to explain it.
171 Percolation thresholds can also be generated by models that have some kind of memory (Hinrichsen, 2000;
172 Ódor, 2004): for example, a patch that has been exploited for many years will recover differently than a
173 recently deforested forest patch. In this case, the system could belong to a different universality class, or in
174 some cases there is no universality, in which case the value of α will depend on the parameters and details
175 of the model (Corrado, Cherubini, & Pennetta, 2014).

176 To illustrate these concepts, we conducted simulations with a simple forest model with only two states: forest
177 and non-forest. This type of model is called a “contact process” and was introduced for epidemics (Harris,
178 1974), but has many applications in ecology (Gastner et al., 2009; Ricard V. Solé & Bascompte, 2006). A
179 site with forest can become extinct with probability e , and produce another forest site in a neighborhood
180 with probability c . We use a neighborhood defined by an isotropic power law probability distribution. We
181 defined a single control parameter as $\lambda = c/e$ and ran simulations for the subcritical fragmentation state
182 $\lambda < \lambda_c$, with $\lambda = 2$, near the critical point for $\lambda = 2.5$, and for the supercritical state with $\lambda = 5$ (see
183 supplementary data, gif animations).

184 **Patch size distributions**

185 We fitted the empirical distribution of forest patches calculated for each of the thresholds on the range
186 we previously mentioned. We used maximum likelihood (Clauset, Shalizi, & Newman, 2009; Goldstein,
187 Morris, & Yen, 2004) to fit four distributions: power-law, power-law with exponential cut-off, log-normal,
188 and exponential. We assumed that the patch size distribution is a continuous variable that was discretized
189 by remote sensing data acquisition procedure.

190 We set a minimal patch size (X_{min}) at nine pixels to fit the patch size distributions to avoid artifacts at patch
191 edges due to discretization (Weerman et al., 2012). Besides this hard X_{min} limit we set due to discretization,
192 the power-law distribution needs a lower bound for its scaling behavior. This lower bound is also estimated
193 from the data by maximizing the Kolmogorov-Smirnov (KS) statistic, computed by comparing the empirical
194 and fitted cumulative distribution functions (Clauset et al., 2009). For the log-normal model we constrain
195 the values of the μ parameter to positive values, this parameter controls the mode of the distribution and
196 when is negative most of the probability density of the distribution lies outside the range of the forest patch
197 size data (Limpert, Stahel, & Abbt, 2001).

198 To select the best model we calculated corrected Akaike Information Criteria (AIC_c) and Akaike weights for
199 each model (Burnham & Anderson, 2002). Akaike weights (w_i) are the weight of evidence in favor of model
200 i being the actual best model given that one of the N models must be the best model for that set of N
201 models. Additionally, we computed a likelihood ratio test (Clauset et al., 2009; Vuong, 1989) of the power
202 law model against the other distributions. We calculated bootstrapped 95% confidence intervals (Crawley,
203 2012) for the parameters of the best model; using the bias-corrected and accelerated (BCa) bootstrap (Efron
204 & Tibshirani, 1994) with 10000 replications.

205 **Largest patch dynamics**

206 The largest patch is the one that connects the highest number of sites in the area. This has been used
207 extensively to indicate fragmentation (R. H. Gardner & Urban, 2007; Ochoa-Quintero et al., 2015). The
208 relation of the size of the largest patch S_{max} to critical transitions has been extensively studied in relation
209 to percolation phenomena (Bazant, 2000; Botet & Ploszajczak, 2004; Stauffer & Aharony, 1994), but seldom
210 used in ecological studies (for an exception see Gastner et al. (2009)). When the system is in a connected
211 state ($p > p_c$) the landscape is almost insensitive to the loss of a small fraction of forest, but close to the
212 critical point a minor loss can have important effects (B. Oborny et al., 2007; Ricard V. Solé & Bascompte,
213 2006), because at this point the largest patch will have a filamentary structure, i.e. extended forest areas

214 will be connected by thin threads. Small losses can thus produce large fluctuations.

215 One way to evaluate the fragmentation of the forest is to calculate the proportion of the largest patch
216 against the total area (T. H. Keitt, Urban, & Milne, 1997). The total area of the regions we are considering
217 (Appendix S4, figures S1-S6) may not be the same than the total area that the forest could potentially
218 occupy, thus a more accurate way to evaluate the weight of S_{max} is to use the total forest area, that can
219 be easily calculated summing all the forest pixels. We calculate the proportion of the largest patch for each
220 year, dividing S_{max} by the total forest area of the same year: $RS_{max} = S_{max} / \sum_i S_i$. This has the effect of
221 reducing the S_{max} fluctuations produced due to environmental or climatic changes influences in total forest
222 area. When the proportion RS_{max} is large (more than 60%) the largest patch contains most of the forest
223 so there are fewer small forest patches and the system is probably in a connected phase. Conversely, when
224 it is low (less than 20%), the system is probably in a fragmented phase (Saravia & Momo, 2017). As we
225 calculated these largest patch indices for different thresholds, the values of the total forest area and the value
226 of S_{max} are lower as threshold is higher, we expect that the value of RS_{max} will change and probably be
227 lower at high thresholds. To define if a region will be in a connected or unconnected state we used the RS_{max}
228 of the highest threshold (40%) which is more conservative to evaluate the risk of fragmentation and includes
229 the most dense forest area. Additionally if RS_{max} is a good indicator of the fragmented or unfragmented
230 state of the forest and these are the two alternative states for the critical transition the RS_{max} distribution
231 of frequencies should be bimodal (Brandon T. Bestelmeyer et al., 2011); so we apply the Hartigan's dip test
232 that measures departures from unimodality (J. A. Hartigan & Hartigan, 1985).

233 The RS_{max} is a useful qualitative index that does not tell us if the system is near or far from the critical
234 transition; this can be evaluated using the temporal fluctuations. We calculate the fluctuations around the
235 mean with the absolute values $\Delta S_{max} = S_{max}(t) - \langle S_{max} \rangle$, using the proportions of RS_{max} . To characterize
236 fluctuations we fitted three empirical distributions: power-law, log-normal, and exponential, using the same
237 methods described previously. We expect that large fluctuation near a critical point have heavy tails (log-
238 normal or power-law) and that fluctuations far from a critical point have exponential tails, corresponding to
239 Gaussian processes (Rooij, Nash, Rajaraman, & Holden, 2013). As the data set spans 16 years, it is probable
240 that will do not have enough power to reliably detect which distribution is better (Clauset et al., 2009). To
241 improve this we used the same likelihood ratio test we used previously (Clauset et al., 2009; Vuong, 1989);
242 if the p-value obtained to compare the best distribution against the others we concluded that there is not
243 enough data to decide which is the best model. We generated animated maps showing the fluctuations of
244 the two largest patches at 30% threshold, to aid in the interpretations of the results.

245 A robust way to detect if the system is near a critical transition is to analyze the increase in variance of

the density (Benedetti-Cecchi, Tamburello, Maggi, & Bulleri, 2015). It has been demonstrated that the variance increase in density appears when the system is very close to the transition (Corrado et al., 2014), thus practically it does not constitute an early warning indicator. An alternative is to analyze the variance of the fluctuations of the largest patch ΔS_{max} : the maximum is attained at the critical point but a significant increase occurs well before the system reaches the critical point (Corrado et al., 2014; Saravia & Momo, 2017). In addition, before the critical fragmentation, the skewness of the distribution of ΔS_{max} should be negative, implying that fluctuations below the average are more frequent. We characterized the increase in the variance using quantile regression: if variance is increasing the slopes of upper or/and lower quartiles should be positive or negative.

All statistical analyses were performed using the GNU R version 3.3.0 (R Core Team, 2015), to fit the distributions of patch sizes we used the Python package powerlaw (Alstott, Bullmore, & Plenz, 2014). For the quantile regressions we used the R package quantreg (Koenker, 2016). Image processing was done in MATLAB r2015b (The Mathworks Inc.). The complete source code for image processing and statistical analysis, and the patch size data files are available at figshare <http://dx.doi.org/10.6084/m9.figshare.4263905>.

Results

The figure 1 shows an example of the distribution of the biggest 200 patches for years 2000 and 2014, this distribution is highly variable, but the biggest patch usually maintains its place. Sometimes the biggest patch breaks and then big fluctuations in its size are observed, as we will analyze below. Smaller patches can merge or break more easily so they enter or leave the list of 200, and this is why there is a color change across years.

The power law distribution was selected as the best model in 99% of the cases (Figure S7). In a small number of cases (1%) the power law with exponential cutoff was selected, but the value of the parameter α was similar by ± 0.03 to the pure power law (Table S1, and model fit data table). Additionally the patch size where the exponential tail begins is very large, thus we used the power law parameters for this cases (region EUAS3,SAST2). In finite-size systems the favored model should be the power law with exponential cut-off, because the power-law tails are truncated to the size of the system (Stauffer & Aharony, 1994). This implies that differences between the two kinds of power law models should be small. We observed that phenomena: when the pure power-law model is selected as the best model the likelihood ratio test shows that in 64% of the cases the differences with power law with exponential cutoff are not significant ($p\text{-value}>0.05$); in these cases the differences between the fitted α for both models are less than 0.001. Instead the likelihood ratio

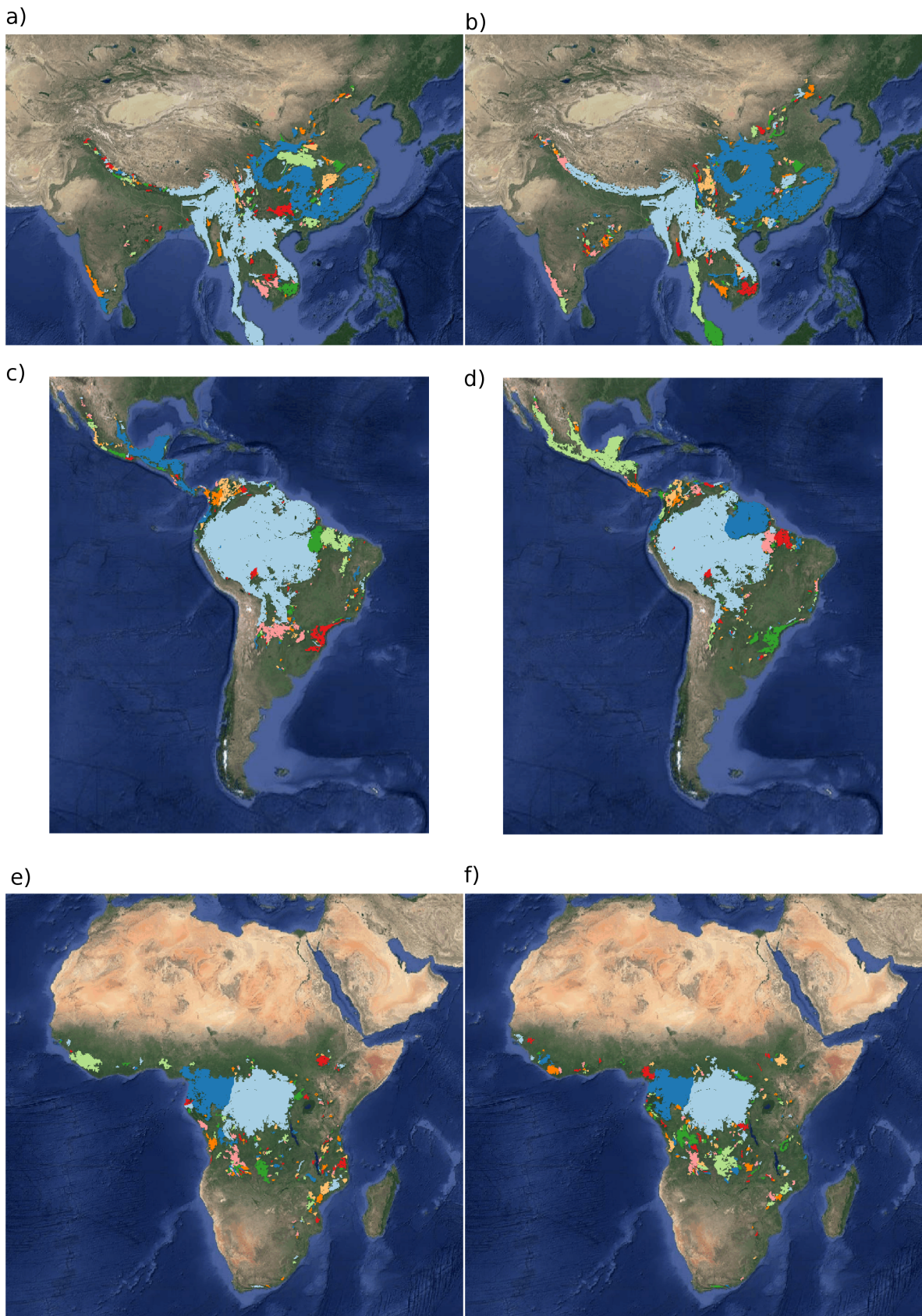


Figure 1: Forest patch distributions for continental regions for the years 2000 and 2014. The images are the 200 biggest patches, showed at a coarse pixel scale of 2.5 km. The regions are: a) & b) southeast Asia; c) & d) South America subtropical and tropical and e) & f) Africa mainland, for the years 2000 and 2014 respectively. The color palette was chosen to discriminate different patches and do not represent patch size.

276 test clearly differentiates the power law model from the exponential model (100% cases p-value<0.05), and
277 the log-normal model (90% cases p-value<0.05).

278 The global mean of the power-law exponent α is 1.967 and the bootstrapped 95% confidence interval is 1.964
279 - 1.970. Besides that, the global values for each threshold are different, because their confidence intervals
280 do not overlap, and their range goes from 1.90 to 2.01 (Table S1). Analyzing the biggest regions (Figure
281 1, Table S2) the north hemisphere (EUAS1 & NA1) have similar values of α (1.97, 1.98), pantropical areas
282 have different α with greatest values for South America (SAST1, 2.01) and in descending order Africa (AF1,
283 1.946) and Southeast Asia (SEAS1, 1.895). With greater α the fluctuations of patch sizes are lower and vice
284 versa (M. E. J. Newman, 2005).

285 We calculated the total areas of forest and the largest patch S_{max} by year for different thresholds; as expected
286 these two values increase for smaller thresholds (Table S3). We expect less variations in the largest patch
287 relative to total forest area RS_{max} (Figure S9); in ten cases it keeps near or higher than 60% (EUAS2, NA5,
288 OC2, OC3, OC4, OC5, OC6, OC8, SAST1, SAT1) over the 25-35 range or more. In four cases it keeps
289 around 40% or less at least over the 25-30% range (AF1, EUAS3, OC1, SAST2) and in six cases there is
290 a crossover from more than 60% to around 40% or less (AF2, EUAS1, NA1, OC7, SEAS1, SEAS2). This
291 confirms the criteria of using the most conservative threshold value of 40% to interpret RS_{max} with regard
292 to the fragmentation state of the forest. The frequency of RS_{max} showed bimodality (Figure 3) and the dip
293 test rejected unimodality ($D = 0.0416$, p-value = 0.0003), which also indicates RS_{max} as a good index to
294 study the fragmentation state of the forest.

295 The RS_{max} for regions with more than 10^7 km² of forest is shown in figure 4. South America tropical and
296 subtropical (SAST1) is the only region with an average close to 60%, the other regions are below 30%. Eurasia
297 mainland (EUAS1) has the lowest value near 20%. For regions with less total forest area (Figure S10, Table
298 S3), Great Britain (EUAS3) has the lowest proportion less than 5%, Java (OC7) and Cuba (SAST2) are
299 under 25%, while other regions such as New Guinea (OC2), Malaysia/Kalimantan (OC3), Sumatra (OC4),
300 Sulawesi (OC5) and South New Zealand (OC6) have a very high proportion (75% or more). Philippines
301 (SEAS2) seems to be a very interesting case because it seems to be under 30% until the year 2007, fluctuates
302 around 30% in years 2008-2010, then jumps near 60% in 2011-2013 and then falls again to 30%, this seems
303 an example of a transition from a fragmented state to a unfragmented one (figure S10).

304 We analyzed the distributions of fluctuations of the largest patch relative to total forest area ΔRS_{max} and
305 the fluctuations of the largest patch ΔS_{max} . Besides the Akaike criteria identified different distributions as
306 the best, in most cases the Likelihood ratio test is not significant thus the data is not enough to determine

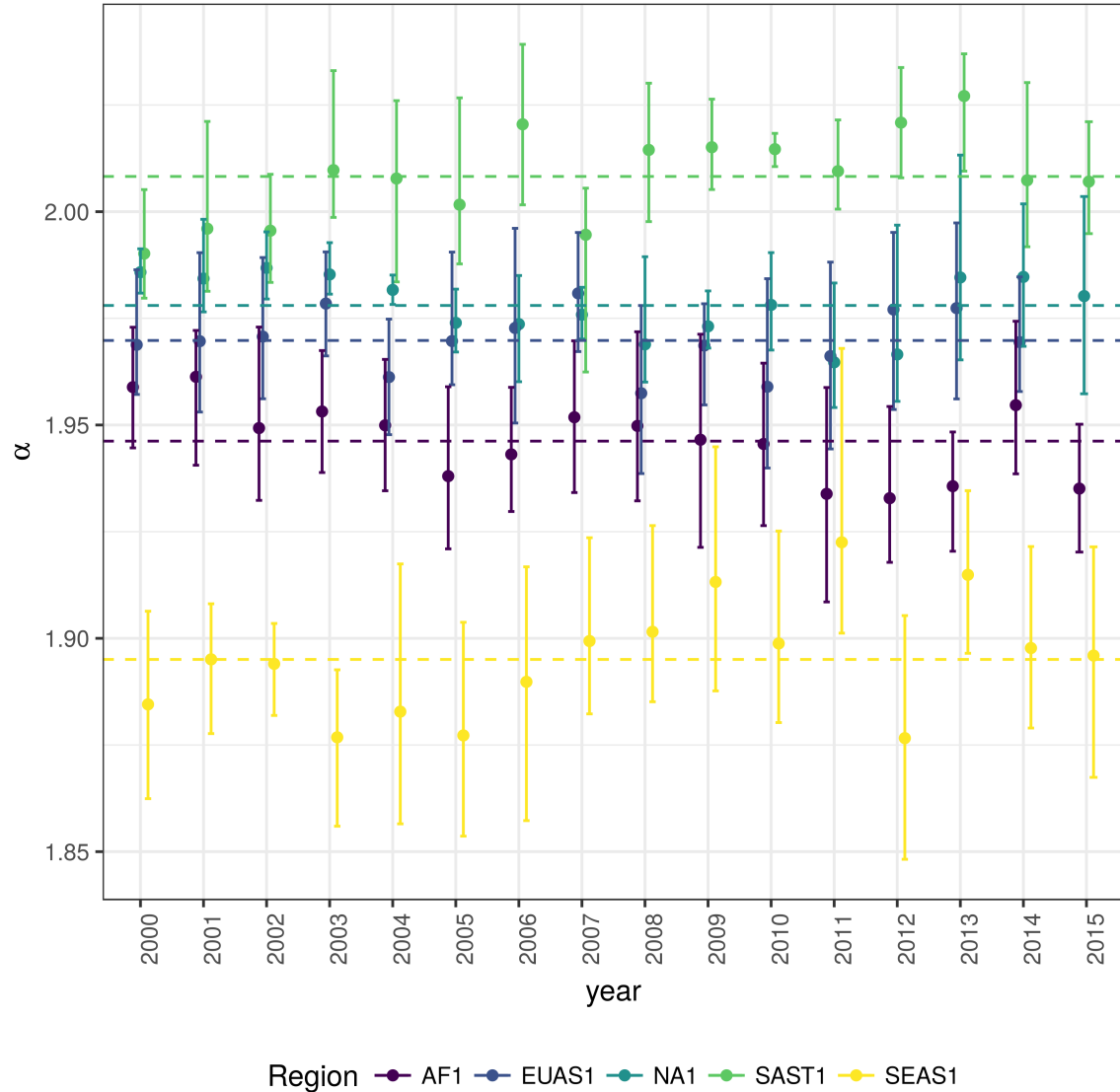


Figure 2: Power law exponents (α) of forest patch distributions for regions with total forest area $> 10^7 \text{ km}^2$. Dashed horizontal lines are the means by region, with 95% confidence interval error bars estimated by bootstrap resampling. The regions are AF1: Africa mainland, EUAS1: Eurasia mainland, NA1: North America mainland, SAST1: South America subtropical and tropical, SEAS1: Southeast Asia mainland.

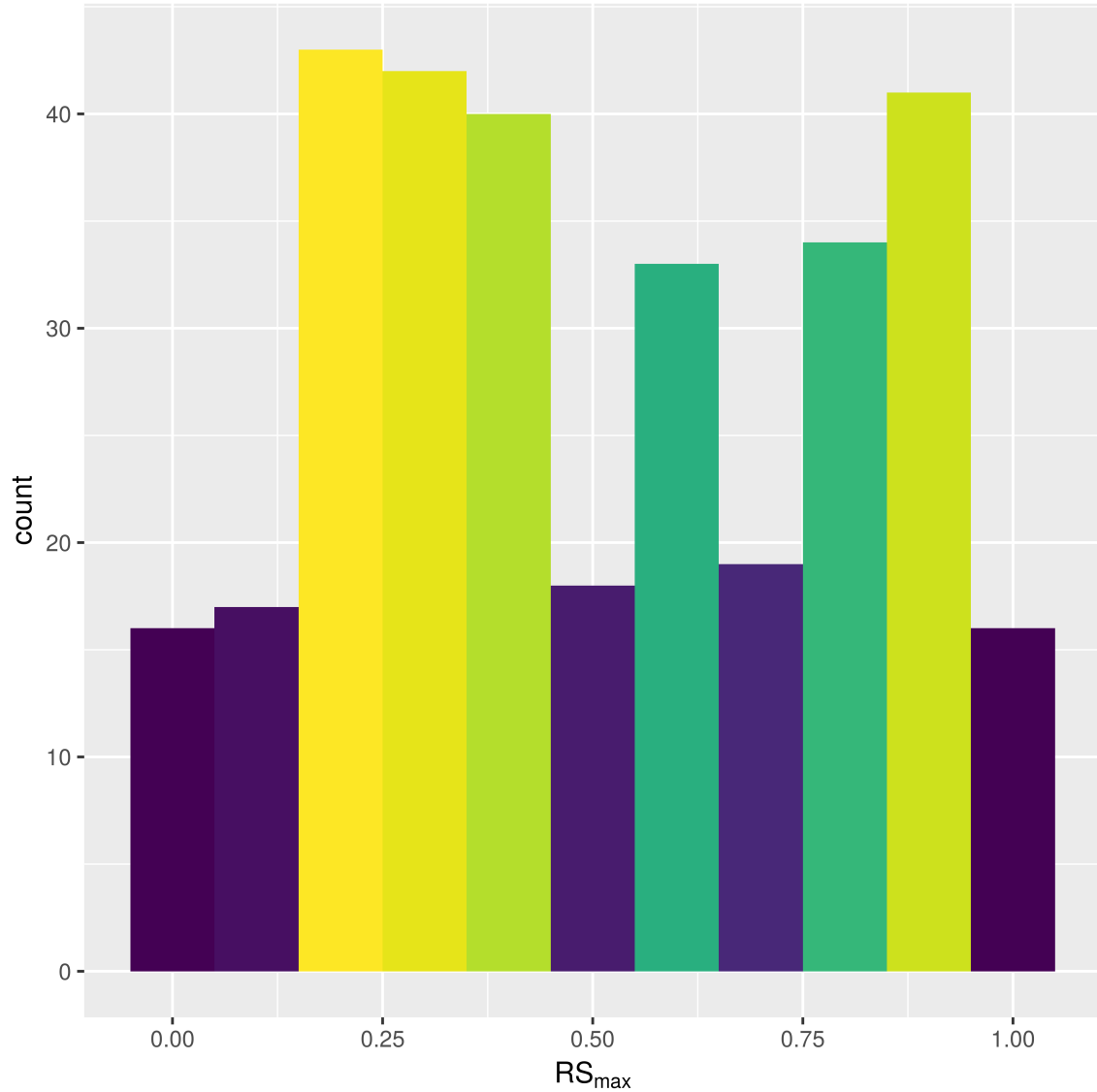


Figure 3: Frequency distribution of Largest patch proportion relative to total forest area RS_{max} calculated using a threshold of 40% of forest in each pixel to determine patches. Bimodality is observed and confirmed by the dip test ($D = 0.0416$, $p\text{-value} = 0.0003$). This indicates the existence of two states needed for a critical transition.

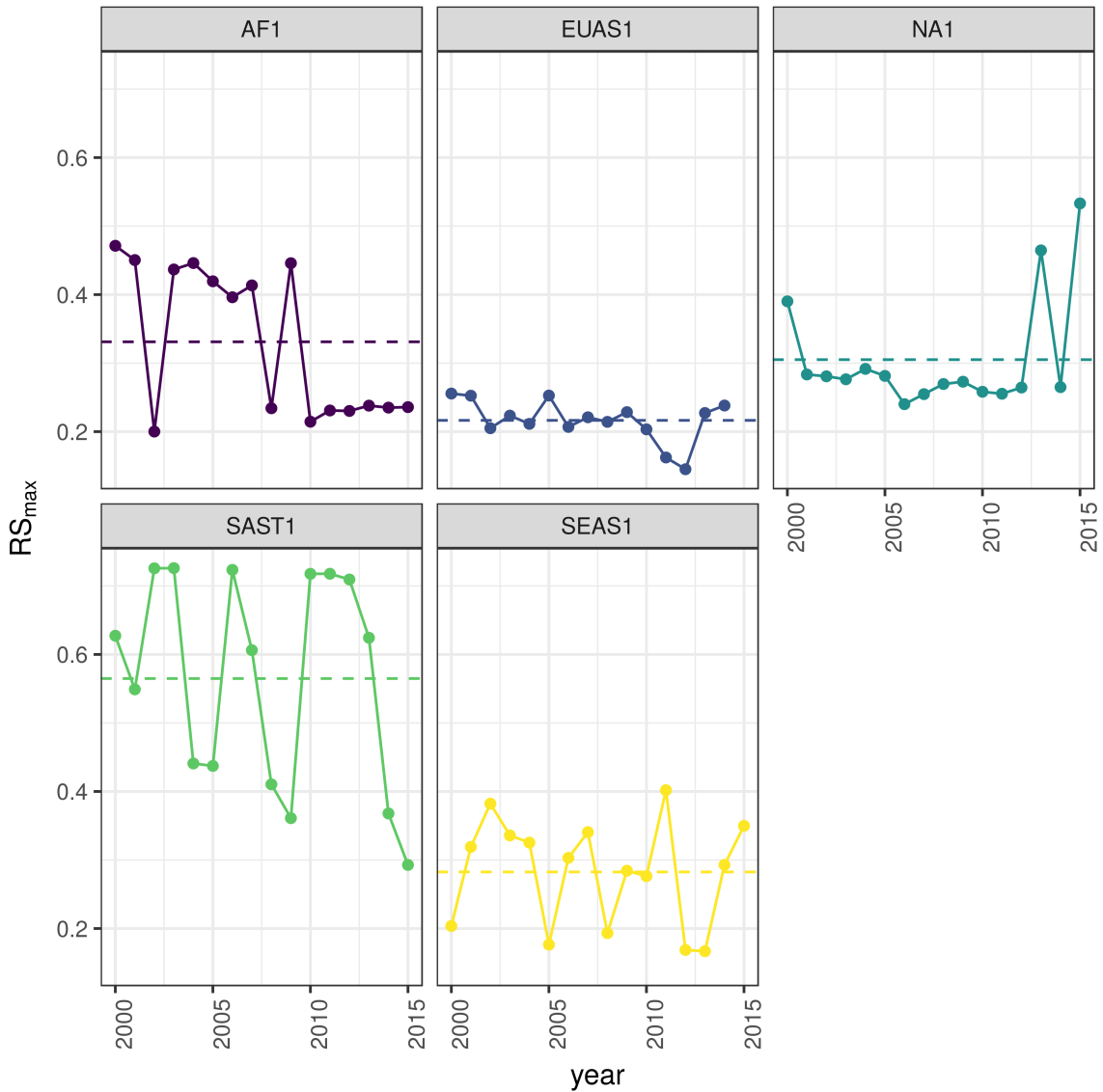


Figure 4: Largest patch proportion relative to total forest area RS_{max} , for regions with total forest area $> 10^7 \text{ km}^2$. We show here the RS_{max} calculated using a threshold of 40% of forest in each pixel to determine patches. Dashed lines are averages across time. The regions are AF1: Africa mainland, EUAS1: Eurasia mainland, NA1: North America mainland, SAST1: South America tropical and subtropical, SEAS1: Southeast Asia mainland.

307 with confidence which is the best distribution. Only 1 case the distribution selected by the Akaike criteria is
308 confirmed as the correct model for relative and absolute fluctuations (Table S4). Thus we do not apply this
309 criteria because is not informative, we can not decide with reliability if the best distribution is the selected
310 one.

311 The animations of the two largest patches (see supplementary data, largest patch gif animations) qualitatively
312 shows the nature of fluctuations and if the state of the forest is connected or not. If the largest patch is
313 always the same patch over time, the forest is probably not fragmented; this happens for regions with RS_{max}
314 of more than 40% such as AF2 (Madagascar), EUAS2 (Japan), NA5 (Newfoundland) and OC3 (Malaysia).
315 In the regions with RS_{max} between 40% and 30% the identity of the largest patch could change or stay the
316 same in time. For OC7 (Java) the largest patch changes and for AF1 (Africa mainland) it stays the same.
317 Only for EUAS1 (Eurasia mainland) we observed that the two largest patches are always the same, implying
318 that this region is probably composed of two independent domains and should be divided in further studies.
319 The regions with RS_{max} less than 25%: SAST2 (Cuba) and EUAS3 (Great Britain), the largest patch always
320 changes reflecting their fragmented state. In the case of SEAS2 (Philippines) a transition is observed, with
321 the identity of the largest patch first variable, and then constant after 2010.

322 The results of quantile regressions are almost identical for ΔRS_{max} and ΔS_{max} (table S5); in very few cases
323 only one of them is significant but we only take into account results where both are significant. Among the
324 biggest regions, Africa (AF1) has a similar pattern across thresholds but only at 30% threshold is significant;
325 the upper and lower quantiles have significant negative slopes, but the lower quantile slope is lower, implying
326 that negative fluctuations and variance are increasing (Figure 5). Eurasia mainland (EUAS1) has significant
327 slopes at 20%, 30% and 40% thresholds but the patterns are different at 20% variance is decreasing, at 30%
328 and 40% only is increasing. This is because the largest patch is composed of pixels with different cover
329 of forest, thus there are more variation in pixels from 30% to 20% than from 20% to less than 20%, then
330 the fluctuations are happening between 40% and 20%. The signal is that the variation of the most dense
331 portion of the largest patch is increasing within a limited range. North America mainland (NA1) exhibits
332 the same pattern at 20%, 25% and 30% thresholds: a significant lower quantile with positive slope, implying
333 decreasing variance. South America tropical and subtropical (SAST1) have significant lower quantile with
334 negative slope at 25% and 30% thresholds indicating an increase in variance. Finally, SEAS1 have a upper
335 quantile with positive slope significant for 25% threshold, also indicating an increasing variance. The other
336 regions, with forest area smaller than 10^7 km^2 are showed in figure S11 and table S5. Philippines (SEAS2)
337 is an interesting case: the slopes of lower quantils are positive for thresholds 20% and 25%, and the upper
338 quantil slopes are positive for thresholds 30% and 40%; thus variance is decreasing at 20%-25% and increasing

339 at 30%-40%.

340 The conditions that indicate that a region is near a critical fragmentation threshold are that patch size
 341 distributions follow a power law; variance of ΔRS_{max} is increasing in time; and skewness is negative. All
 342 these conditions must happen at the same time at least for one threshold. When the threshold is higher more
 343 dense regions of the forest are at risk. This happens for Africa mainland (AF1), Eurasia mainland(EUAS1),
 344 Japan (EUAS2), Australia mainland (OC1), Malaysia/Kalimantan (OC3), Sumatra (OC4), South America
 345 tropical & subtropical (SAST1), Cuba (SAST2), Southeast Asia, Mainland (SEAS1).

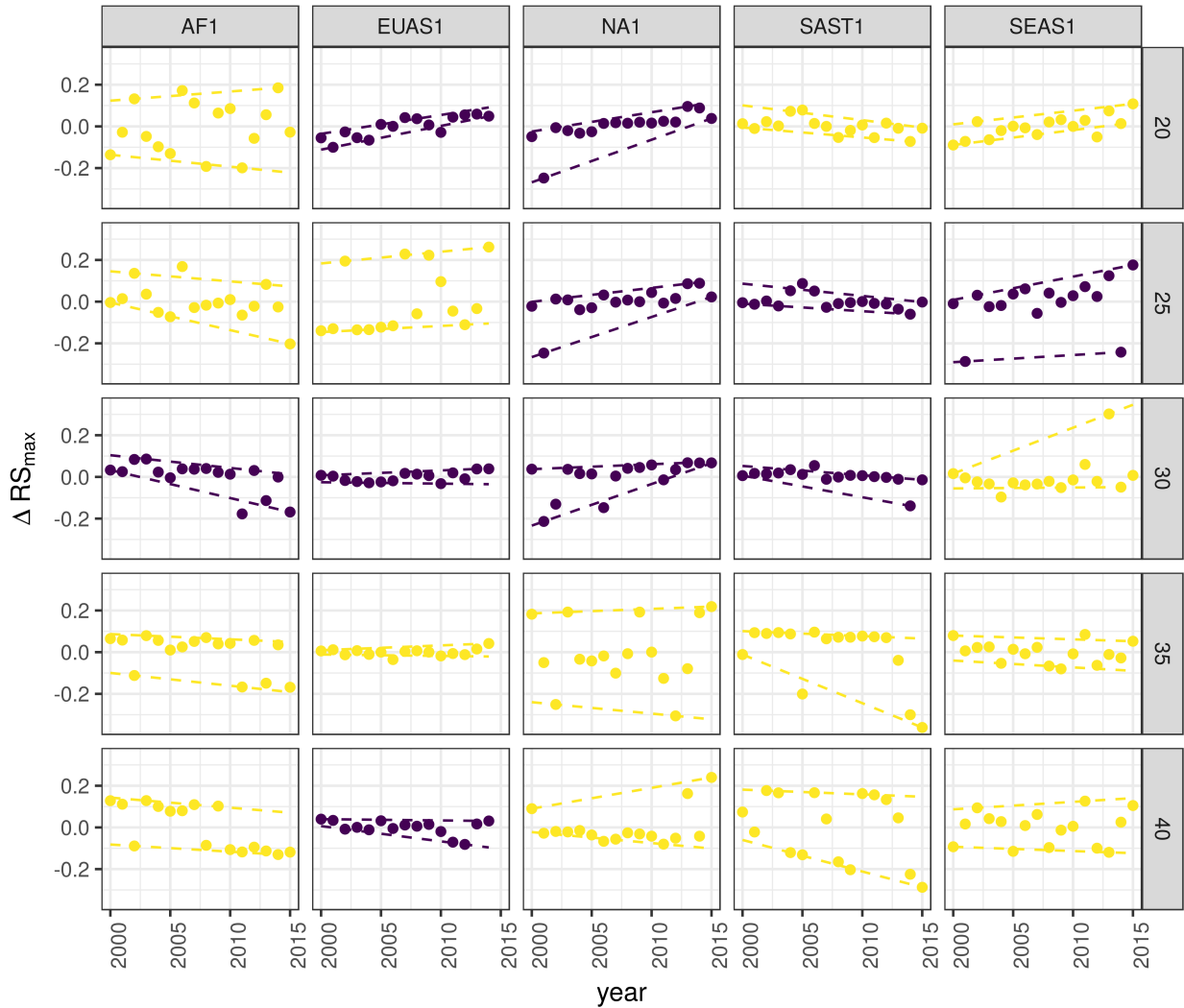


Figure 5: Largest patch fluctuations for regions with total forest area $> 10^7 \text{ km}^2$ across years. The patch sizes are relative to the total forest area of the same year. Dashed lines are 90% and 10% quantile regressions, to show if fluctuations were increasing; purple (dark) panels have significant slopes. The regions are AF1: Africa mainland, EUAS1: Eurasia mainland, NA1: North America mainland, SAST1: South America tropical and subtropical, SEAS1: Southeast Asia mainland.

Table 1: Regions and indicators of closeness to a critical fragmentation point. Where: RS_{max} is the largest patch divided by the total forest area; Threshold is the value used to calculate patches from the MODIS VCF pixels; ΔRS_{max} are the fluctuations of RS_{max} around the mean and the increase or decrease in the variance was estimated using quantile regressions; skewness was calculated for RS_{max} . NS means the results were non-significant. The conditions that determine the closeness to a fragmentation point are: increasing variance of ΔRS_{max} and negative skewness. RS_{max} indicates if the forest is unfragmented (>0.6) or fragmented (<0.3).

Region	Description	RS_{max}	Threshold	Variance of ΔRS_{max}	Skewness
AF1	Africa mainland	0.33	30	Increase	-1.4653
AF2	Madagascar	0.48	20	Increase	0.7226
EUAS1	Eurasia, mainland	0.22	20	Decrease	-0.4814
EUAS1			30	Increase	0.3113
EUAS1			40	Increase	-1.2790
EUAS2	Japan	0.94	35	Increase	-0.3913
EUAS2			40	Increase	-0.5030
EUAS3	Great Britain	0.03	40	NS	
NA1	North America, mainland	0.31	20	Decrease	-2.2895
NA1			25	Decrease	-2.4465
NA1			30	Decrease	-1.6340
NA5	Newfoundland	0.54	40	NS	
OC1	Australia, Mainland	0.36	30	Increase	0.0920
OC1			35	Increase	-0.8033
OC2	New Guinea	0.96	25	Decrease	-0.1003
OC2			30	Decrease	0.1214
OC2			35	Decrease	-0.0124
OC3	Malaysia/Kalimantan	0.92	35	Increase	-1.0147
OC3			40	Increase	-1.5649
OC4	Sumatra	0.84	20	Increase	-1.3846
OC4			25	Increase	-0.5887
OC4			30	Increase	-1.4226
OC5	Sulawesi	0.82	40	NS	
OC6	New Zealand South Island	0.75	40	Increase	0.3553
OC7	Java	0.16	40	NS	
OC8	New Zealand North Island	0.64	40	NS	
SAST1	South America, Tropical and Subtropical forest	0.56	25	Increase	1.0519
SAST1			30	Increase	-2.7216
SAST2	Cuba	0.15	20	Increase	0.5049
SAST2			25	Increase	1.7263
SAST2			30	Increase	0.1665
SAST2			40	Increase	-0.5401
SAT1	South America, Temperate forest	0.54	25	Decrease	0.1483
SAT1			30	Decrease	-1.6059
SAT1			35	Decrease	-1.3809
SEAS1	Southeast Asia, Mainland	0.28	25	Increase	-1.3328
SEAS2	Philippines	0.33	20	Decrease	-1.6373
SEAS2			25	Decrease	-0.6648
SEAS2			30	Increase	0.1517

Region	Description	RS_{max}	Threshold	Variance of ΔRS_{max}	Skewness
SEAS2			40	Increase	1.5996

346 Discussion

347 We found that the forest patch distribution of all regions of the world followed power laws spanning seven
 348 orders of magnitude. These include tropical rainforest, boreal and temperate forest. Power laws have
 349 previously been found for several kinds of vegetation, but never at global scales as in this study. Moreover
 350 the range of the estimated power law exponents is relatively narrow besides we used different thresholds
 351 (1.90 - 2.01). This suggest the existence of one unifying mechanism or different mechanism that act in the
 352 same way in different regions.

353 Several mechanisms have been proposed for the emergence of power laws in forest: the first is related self
 354 organized criticality (SOC), when the system is driven by its internal dynamics to a critical state; this has
 355 been suggested mainly for fire-driven forests (Hantson, Pueyo, & Chuvieco, 2015; Zinck & Grimm, 2009).
 356 Real ecosystems do not seem to meet the requirements of SOC dynamics because their are driven both
 357 endogenous and exogenous controls, non-homogeneous and they may not have the separation of time scales
 358 [Ricard V Solé, Alonso, & Mckane (2002);Sole2006]; furthermore there is some evidence that these conditions
 359 are not meet (McKenzie & Kennedy, 2012; S. Pueyo et al., 2010). A second possible mechanism, suggested
 360 by Pueyo et al. (2010), is isotropic percolation, when a system is near the critical point power law structures
 361 arise. This is equivalent to the random forest model that we explained previously, and requires the tuning
 362 of an external environmental condition to carry the system to this point. We did not expect forest growth
 363 to be a random process at local scales, but it is possible that combinations of factors cancel out to produce
 364 seemingly random forest dynamics at large scales. In this case we should have observed power laws in a
 365 limited set of situations that coincide with a critical point and we observed pervasive power law distributions
 366 thus percolation is not the mechanisms that produce the observed distributions. This does not mean that
 367 second order critical transitions are not present but that we can not detect them by means of patch size
 368 distributions. The third mechanism suggested as the cause of pervasive power laws in patch size distribution
 369 is facilitation (Irvine, Bull, & Keeling, 2016; Manor & Shnerb, 2008): a patch surrounded by forest will have
 370 a smaller probability of been deforested or degraded than an isolated patch. We hypothesize that models
 371 that include facilitation could explain the patterns observed here. The model of Scanlon et al. (2007) showed
 372 an $\alpha = 1.34$ which is different from our results (1.90 - 2.01 range). Another model but with three states
 373 (tree/non-tree/degraded), including local facilitation and grazing, was also used to obtain power laws patch

374 distributions without external tuning, and exhibited deviations from power laws at high grazing pressures
375 (S. Kéfi et al., 2007). The values of the power law exponent α obtained for this model are dependent on the
376 intensity of facilitation, when facilitation is more intense the exponent is higher, but the maximal values they
377 obtained are still lower than the ones we observed. The interesting point is that the value of the exponent is
378 dependent on the parameters, and thus the observed α might be obtained with some parameter combination.

379 The existence of a critical transitions in forest, mainly in neotropical forest to savanna, is a matter of intense
380 investigation, this is in general thought as first order or discontinuous transitions; we found power laws in
381 forest patch distributions which is a necessary but not a sufficient condition for a second order or continuous
382 transition. Moreover, a power law patch distribution can be indicative of a critical transition if it is present
383 in a narrow range of conditions; conversely if it is not found, the existence of a critical transition cannot be
384 discarded. Regardless this, new research suggested that first order transitions do not even exists when the
385 system is spatially heterogeneous and present internal and external stochastic fluctuations as in forest; thus
386 the application of indices based on second order transitions seems to be justified.

387 It has been suggested that a combination of spatial and temporal indicators could more reliably detect
388 critical transitions (S. Kéfi et al., 2014). In this study, we combined five criteria to detect the closeness to
389 a fragmentation threshold. Two of them were spatial: the forest patch size distribution, and the proportion
390 of the largest patch relative to total forest area RS_{max} . The other three were the distribution of temporal
391 fluctuations in the largest patch size, the trend in the variance, and the skewness of the fluctuations. One
392 of them: the distribution of temporal fluctuations ΔRS_{max} can not be applied with our temporal resolution
393 due to the difficulties of fitting and comparing heavy tailed distributions. The combination of the remaining
394 four gives us an increased degree of confidence about the system being close to a critical transition.

395 The monitoring of biggest patches using RS_{max} is also important regardless the existence or not of critical
396 transitions. RS_{max} could be used to compare regions with different forest extension and as the total area
397 of forest also change with different environmental condition is at least partially independent of climatic
398 conditions could be also applied to compare forest from different latitudes. Moreover, RS_{max} contain most
399 of the intact forest landscapes defined by P. Potapov et al. (2008), thus it is a relatively simple way to
400 evaluate the risk in these areas.

401 We found that several continental areas and islands met our criteria, this analysis is at scale of continents so
402 it is in fact a macrosystems perspective (Heffernan et al., 2014). In a macrosystems analysis it is important
403 to link the local processes that produce the continental patterns, what we did here is to find the macro scale
404 dynamical patterns that deserve attention. To link these patterns across scales requires a substantial amount

405 of investigation, probably performing the same analysis for smaller regions that identify more clearly which
406 kind of forest and processes are locally involved. We know that the same procedure could be applied to local
407 scales because the patch distributions are power laws; power law distributions are self-similar, or invariant
408 to scale changes. Thus unless power law distribution are broken we could apply the same methodology to
409 more local scales.

410 South America tropical and subtropical (SAST1), Southeast Asia mainland (SEAS1) and Africa mainland
411 (AF1) met all criteria at least for one threshold; this regions experience the biggest rates of deforestation
412 with a significant increase in loss of forest (M. C. Hansen et al., 2013). From our point of view the region
413 most critical is the Southeast Asia because the proportion of the largest patch relative to total forest area
414 RS_{max} 28%, then Africa with 33% and then South America with 56%. This is indicating that Southeast
415 Asia is the most fragmented and thus the most endangered region. Due to the criteria we adopted to defined
416 regions, we can not detect the effect of conservation policies applied at a country level, e.g. the Natural
417 Forest Conservation Program in China, which produced an 1.6% increase in forest cover and net primary
418 productivity (Viña, McConnell, Yang, Xu, & Liu, 2016).

419 Indonesia and Malaysia (OC3) both are countries with hight deforestation rates (M. C. Hansen et al., 2013);
420 Sumatra (OC4) is the biggest island of Indonesia and where most deforestation occurs. Both regions show
421 a high RS_{max} greater than 60% thus the forest is in an unfragmented state but they met all criteria, thus
422 this means that they are approaching a transition if the actual deforestation rates continue. At present our
423 indices are qualitative but we expect to develop them in a more quantitative way to predict how many years
424 would be needed to complete a critical transition if actual forest loss rates are maintained.

425 The eurasian mainland region (EUAS1) is an extensive area with mainly temperate and boreal forest, and a
426 combination of forest loss due to fire (P. Potapov, Hansen, Stehman, Loveland, & Pittman, 2008) and forestry.
427 The biggest country is Russia that experienced the biggest rate of forest loss of all countries, but here in
428 the zone of coniferous forest the the largest gain is observed due to agricultural abandonment (Prishchepov,
429 Müller, Dubinin, Baumann, & Radeloff, 2013). The loss is maximum at the most dense areas of forest (M.
430 C. Hansen et al., 2013, Table S3), this coincides with our analysis that detect an increasing risk at denser
431 forest. This region also has a relatively low RS_{max} that means is probably near a fragmented state.

432 A region that is similar in forest composition to EAUS1 is North America (NA1); the two main countries
433 involved, United States and Canada, are also in the first places of forest loss, with forest dynamics also
434 mainly influenced by fire and forestry. Both regions are extensively managed for wood for industrial wood
435 production, North America have a higher RS_{max} than eurasia and a positive skewness that excludes it from

436 beeing near a critical transition. A possible explanation of this is that in Russia after the collapse of the
437 Soviet Union harvest was lower due to agricultural abandonment but illegal overharvesting of high valued
438 stands increased (Gauthier, Bernier, Kuuluvainen, Shvidenko, & Schepaschenko, 2015) and that could be
439 the cause of the differences we found between them.

440 The analysis of RS_{max} reveals that the island of Philippines (SEAS2) seems to be an example of a critical
441 transition from an unconnected to a connected state, it can be qualitatively observed a transition from a state
442 with high fluctuations and low RS_{max} to a state with low fluctuations and a high RS_{max} . If we observe this
443 pattern backwards in time: the decrease in variance becomes and increase and negative skewness maintains
444 the same, thus the region would show the criteria of a critical transition (Table 1, Figure S11). The actual
445 pattern of transition to an unfragmented state could be the result of an active intervention of the government
446 promoting conservation and rehabilitation of protected areas, ban of logging old-growth forest, reforestation
447 of barren areas, community-based forestry activities, and sustainable forest management in the country's
448 production forest (Lasco et al., 2008). This confirms that the early warning indicators proposed here work
449 in the correct direction. The MODIS dataset does not detect if native forest is replaced by agroindustrial
450 tree plantations like oil palms, that are among the main drivers of deforestation in this area (Malhi, Gardner,
451 Goldsmith, Silman, & Zelazowski, 2014). To improve the estimation of forest patches, data sets as the
452 MODIS cropland probability and others about land use, protected areas, forest type, should be incorporated
453 (M. Hansen et al., 2014; J. O. Sexton et al., 2015).

454 Deforestation and fragmentation are closely related. At low levels of habitat reduction species population
455 will decline proportionally; this can happen even when the habitat fragments retain connectivity. As habi-
456 tation reduction continues, the critical threshold is approached and connectivity will have large fluctuations
457 (Brook, Ellis, Perring, Mackay, & Blomqvist, 2013). This could trigger several negative synergistic effects:
458 populations fluctuations and the possibility of extinctions will rise, increasing patch isolation and decreasing
459 connectivity (Brook et al., 2013). This positive feedback mechanism will be enhanced when the fragmenta-
460 tion threshold is reached, resulting in the loss of most habitat specialist species at a landscape scale (Pardini
461 et al., 2010). Some authors argue that since species have heterogeneous responses to habitat loss and frag-
462 mentation, and biotic dispersal is limited, the importance of thresholds is restricted to local scales or even
463 that its existence is questionable (Brook et al., 2013). Fragmentation is by definition a local process that at
464 some point produces emergent phenomena over the entire landscape, even if the area considered is infinite
465 (B. Oborny, Meszéna, & Szabó, 2005). In addition, after a region's fragmentation threshold connectivity
466 decreases, there is still a large and internally well connected patch that can maintain sensitive species (A. C.
467 Martensen, Ribeiro, Banks-Leite, Prado, & Metzger, 2012). What is the time needed for these large patches

468 to become fragmented, and pose a real danger of extinction to a myriad of sensitive species? If a forest is
469 already in a fragmented state, a second critical transition from forest to non-forest could happen, this was
470 called the desertification transition (Corrado et al., 2014). Considering the actual trends of habitat loss,
471 and studying the dynamics of non-forest patches—instead of the forest patches as we did here—the risk of
472 this kind of transition could be estimated. The simple models proposed previously could also be used to
473 estimate if these thresholds are likely to be continuous and reversible or discontinuous and often irreversible
474 (Weissmann & Shnerb, 2016), and the degree of protection (e.g. using the set-asides strategy Banks-Leite et
475 al. (2014)) than would be necessary to stop this trend.

476 The effectiveness of landscape management is related to the degree of fragmentation, and the criteria to
477 direct reforestation efforts could be focused on regions near a transition (B. Oborny et al., 2007). Regions
478 that are in an unconnected state require large efforts to recover a connected state, but regions that are near
479 a transition could be easily pushed to a connected state; feedbacks due to facilitation mechanisms might
480 help to maintain this state. Crossing the fragmentation critical point in forests could have negative effects
481 on biodiversity and ecosystem services (Haddad et al., 2015), but it could also produce feedback loops at
482 different levels of the biological hierarchy. This means that a critical transition produced at a continental
483 scale could have effects at the level of communities, food webs, populations, phenotypes and genotypes
484 (Barnosky et al., 2012). All these effects interact with climate change, thus there is a potential production of
485 cascading effects that could lead to an abrupt climate change with potentially large ecological and economic
486 impact (Alley et al., 2003).

487 Therefore, even if critical thresholds are reached only in some forest regions at a continental scale, a cascading
488 effect with global consequences could still be produced, and may contribute to reach a planetary tipping point
489 (Reyer, Rammig, Brouwers, & Langerwisch, 2015). The risk of such event will be higher if the dynamics of
490 separate continental regions are coupled (Lenton & Williams, 2013). At least three of the regions defined
491 here are considered tipping elements of the earth climate system that could be triggered during this century
492 (Lenton et al., 2008). These were defined as policy relevant tipping elements so that political decisions could
493 determine whether the critical value is reached or not. Thus using the criteria proposed here could be used
494 as a more sensitive system to evaluate the closeness of a tipping point at a continental scale, but the same
495 criteria could also be used to evaluate local problems at smaller areas. Further improvements will produce
496 quantitative predictions about the temporal horizon where these critical transitions could produce significant
497 changes in the studied systems.

498 **Supporting information**

499 **Appendix**

500 *Table S1:* Mean power-law exponent and Bootstrapped 95% confidence intervals by threshold.

501 *Table S2:* Mean power-law exponent and Bootstrapped 95% confidence intervals across thresholds by region
502 and year.

503 *Table S3:* Mean total patch area; largest patch S_{max} in km²; largest patch proportional to total patch area
504 RS_{max} and 95% bootstrapped confidence interval of RS_{max} , by region and thresholds, averaged across years

505 *Table S4:* Model selection for distributions of fluctuation of largest patch ΔS_{max} and largest patch relative
506 to total forest area ΔRS_{max} .

507 *Table S5:* Quantil regressions of the fluctuations of the largest patch vs year, for 10% and 90% quantils at
508 different pixel thresholds.

509 *Table S6:* Unbiased estimation of Skewness of fluctuations of the largest patch ΔS_{max} and fluctuations
510 relative to total forest area ΔRS_{max} .

511 *Figure S1:* Regions for Africa: Mainland (AF1), Madagascar (AF2).

512 *Figure S2:* Regions for Eurasia: Mainland (EUAS1), Japan (EUAS2), Great Britain (EUAS3).

513 *Figure S3:* Regions for North America: Mainland (NA1), Newfoundland (NA5).

514 *Figure S4:* Regions for Australia and islands: Australia mainland (OC1), New Guinea (OC2),
515 Malaysia/Kalimantan (OC3), Sumatra (OC4), Sulawesi (OC5), New Zealand south island (OC6),
516 Java (OC7), New Zealand north island (OC8).

517 *Figure S5:* Regions for South America: Tropical and subtropical forest up to Mexico (SAST1), Cuba
518 (SAST2), South America Temperate forest (SAT1).

519 *Figure S6:* Regions for Southeast Asia: Mainland (SEAS1), Philippines (SEAS2).

520 *Figure S7:* Proportion of best models selected for patch size distributions using the Akaike criterion.

521 *Figure S8:* Power law exponents for forest patch distributions by year for all regions.

522 *Figure S9:* Average largest patch relative to total forest area RS_{max} by threshold, for all regions.

523 *Figure S10:* Largest patch relative to total forest area RS_{max} by year at 40% threshold, for regions with
524 total forest area less than 10^7 km².

525 *Figure S11*: Fluctuations of largest patch relative to total forest area RS_{max} for regions with total forest
526 area less than 10^7 km^2 by year and threshold.

527 Data Accessibility

528 Csv text file with model fits for patch size distribution, and model selection for all the regions; Gif Animations
529 of a forest model percolation; Gif animations of largest patches; patch size files for all years and regions used
530 here; and all the R, Python and Matlab scripts are available at figshare [http://dx.doi.org/10.6084/m9.
531 figshare.4263905](http://dx.doi.org/10.6084/m9.figshare.4263905).

532 Acknowledgments

533 LAS and SRD are grateful to the National University of General Sarmiento for financial support. We want to
534 thank to Jordi Bascompte, Nara Guisoni, Fernando Momo, and two anonymous reviewers for their comments
535 and discussions that greatly improved the manuscript. This work was partially supported by a grant from
536 CONICET (PIO 144-20140100035-CO).

537 References

- 538 Alley, R. B., Marotzke, J., Nordhaus, W. D., Overpeck, J. T., Peteet, D. M., Pielke, R. A., ... Wallace, J. M.
539 (2003). Abrupt Climate Change. *Science*, 299(5615), 2005–2010. Retrieved from <http://science.sciencemag.org/content/299/5615/2005.abstract>
- 540 Allington, G. R. H., & Valone, T. J. (2010). Reversal of desertification: The role of physical and chemical
541 soil properties. *Journal of Arid Environments*, 74(8), 973–977. doi:10.1016/j.jaridenv.2009.12.005
- 542 Alstott, J., Bullmore, E., & Plenz, D. (2014). powerlaw: A Python Package for Analysis of Heavy-Tailed
543 Distributions. *PLOS ONE*, 9(1), e85777. Retrieved from <https://doi.org/10.1371/journal.pone.0085777>
- 544 Banks-Leite, C., Pardini, R., Tambosi, L. R., Pearse, W. D., Bueno, A. A., Bruscagin, R. T., ... Metzger,
545 J. P. (2014). Using ecological thresholds to evaluate the costs and benefits of set-asides in a biodiversity
546 hotspot. *Science*, 345(6200), 1041–1045. doi:10.1126/science.1255768
- 547 Barnosky, A. D., Hadly, E. A., Bascompte, J., Berlow, E. L., Brown, J. H., Fortelius, M., ... Smith, A. B.
548 (2012). Approaching a state shift in Earth’s biosphere. *Nature*, 486(7401), 52–58. doi:10.1038/nature11018
- 549 Bascompte, J., & Solé, R. V. (1996). Habitat fragmentation and extinction thresholds in spatially explicit

- models. *Journal of Animal Ecology*, 65(4), 465–473. doi:10.2307/5781
- Bazant, M. Z. (2000). Largest cluster in subcritical percolation. *Physical Review E*, 62(2), 1660–1669. Retrieved from <http://link.aps.org/doi/10.1103/PhysRevE.62.1660>
- Belward, A. S. (1996). *The IGBP-DIS Global 1 Km Land Cover Data Set “DISCover”: Proposal and Implementation Plans : Report of the Land Recover Working Group of IGBP-DIS* (p. 61). IGBP-DIS Office. Retrieved from <https://books.google.com.ar/books?id=qixsNAAACAAJ>
- Benedetti-Cecchi, L., Tamburello, L., Maggi, E., & Bulleri, F. (2015). Experimental Perturbations Modify the Performance of Early Warning Indicators of Regime Shift. *Current Biology*, 25(14), 1867–1872. doi:10.1016/j.cub.2015.05.035
- Bestelmeyer, B. T., Duniway, M. C., James, D. K., Burkett, L. M., & Havstad, K. M. (2013). A test of critical thresholds and their indicators in a desertification-prone ecosystem: more resilience than we thought. *Ecology Letters*, 16, 339–345. doi:10.1111/ele.12045
- Bestelmeyer, B. T., Ellison, A. M., Fraser, W. R., Gorman, K. B., Holbrook, S. J., Laney, C. M., ... Sharma, S. (2011). Analysis of abrupt transitions in ecological systems. *Ecosphere*, 2(12), 129. doi:10.1890/ES11-00216.1
- Boettiger, C., & Hastings, A. (2012). Quantifying limits to detection of early warning for critical transitions. *Journal of the Royal Society Interface*, 9(75), 2527–2539. doi:10.1098/rsif.2012.0125
- Bonan, G. B. (2008). Forests and Climate Change: Forcings, Feedbacks, and the Climate Benefits of Forests. *Science*, 320(5882), 1444–1449. doi:10.1126/science.1155121
- Botet, R., & Ploszajczak, M. (2004). Correlations in Finite Systems and Their Universal Scaling Properties. In K. Morawetz (Ed.), *Nonequilibrium physics at short time scales: Formation of correlations* (pp. 445–466). Berlin Heidelberg: Springer-Verlag.
- Brook, B. W., Ellis, E. C., Perring, M. P., Mackay, A. W., & Blomqvist, L. (2013). Does the terrestrial biosphere have planetary tipping points? *Trends in Ecology & Evolution*. doi:10.1016/j.tree.2013.01.016
- Burnham, K., & Anderson, D. R. (2002). *Model selection and multi-model inference: A practical information-theoretic approach* (2nd. ed., p. 512). New York: Springer-Verlag.
- Canfield, D. E., Glazer, A. N., & Falkowski, P. G. (2010). The Evolution and Future of Earth’s Nitrogen Cycle. *Science*, 330(6001), 192–196. doi:10.1126/science.1186120
- Carpenter, S. R., Cole, J. J., Pace, M. L., Batt, R., Brock, W. A., Cline, T., ... Weidel, B. (2011).

- 580 Early Warnings of Regime Shifts: A Whole-Ecosystem Experiment. *Science*, 332(6033), 1079–1082.
581 doi:10.1126/science.1203672
- 582 Clauset, A., Shalizi, C., & Newman, M. (2009). Power-Law Distributions in Empirical Data. *SIAM Review*,
583 51(4), 661–703. doi:10.1137/070710111
- 584 Corrado, R., Cherubini, A. M., & Pennetta, C. (2014). Early warning signals of desertification transitions
585 in semiarid ecosystems. *Physical Review E - Statistical, Nonlinear, and Soft Matter Physics*, 90(6), 62705.
586 doi:10.1103/PhysRevE.90.062705
- 587 Crawley, M. J. (2012). *The R Book* (2nd. ed., p. 1076). Hoboken, NJ, USA: Wiley.
- 588 Crowther, T. W., Glick, H. B., Covey, K. R., Bettigole, C., Maynard, D. S., Thomas, S. M., ... Bradford, M.
589 A. (2015). Mapping tree density at a global scale. *Nature*, 525(7568), 201–205. doi:10.1038/nature14967
- 590 Dai, L., Vorselen, D., Korolev, K. S., & Gore, J. (2012). Generic Indicators for Loss of Resilience Before a
591 Tipping Point Leading to Population Collapse. *Science*, 336(6085), 1175–1177. doi:10.1126/science.1219805
- 592 DiMiceli, C., Carroll, M., Sohlberg, R., Huang, C., Hansen, M., & Townshend, J. (2015). Annual Global Au-
593 tomated MODIS Vegetation Continuous Fields (MOD44B) at 250 m Spatial Resolution for Data Years Begin-
594 ning Day 65, 2000 - 2014, Collection 051 Percent Tree Cover, University of Maryland, College Park, MD, USA.
595 Retrieved from https://lpdaac.usgs.gov/dataset{_}discovery/modis/modis{_}products{_}table/mod44b
- 596 Drake, J. M., & Griffen, B. D. (2010). Early warning signals of extinction in deteriorating environments.
597 *Nature*, 467(7314), 456–459. doi:10.1038/nature09389
- 598 Efron, B., & Tibshirani, R. J. (1994). *An Introduction to the Bootstrap* (p. 456). New York: Taylor &
599 Francis. Retrieved from <https://books.google.es/books?id=gLlpIUXRntoC>
- 600 Filotas, E., Parrott, L., Burton, P. J., Chazdon, R. L., Coates, K. D., Coll, L., ... Messier, C. (2014). Viewing
601 forests through the lens of complex systems science. *Ecosphere*, 5(January), 1–23. doi:10.1890/ES13-00182.1
- 602 Foley, J. A., Ramankutty, N., Brauman, K. A., Cassidy, E. S., Gerber, J. S., Johnston, M., ... Zaks, D. P. M.
603 (2011). Solutions for a cultivated planet. *Nature*, 478(7369), 337–342. doi:10.1038/nature10452
- 604 Folke, C., Jansson, Å., Rockström, J., Olsson, P., Carpenter, S. R., Iii, F. S. C., ... Westley, F. (2011).
605 Reconnecting to the Biosphere. *AMBIO*, 40(7), 719–738. doi:10.1007/s13280-011-0184-y
- 606 Fung, T., O'Dwyer, J. P., Rahman, K. A., Fletcher, C. D., & Chisholm, R. A. (2016). Reproducing static
607 and dynamic biodiversity patterns in tropical forests: the critical role of environmental variance. *Ecology*,

- 608 97(5), 1207–1217. doi:10.1890/15-0984.1
- 609 Gardner, R. H., & Urban, D. L. (2007). Neutral models for testing landscape hypotheses. *Landscape Ecology*,
610 22(1), 15–29. doi:10.1007/s10980-006-9011-4
- 611 Gastner, M. T., Oborny, B., Zimmermann, D. K., & Pruessner, G. (2009). Transition from Connected
612 to Fragmented Vegetation across an Environmental Gradient: Scaling Laws in Ecotone Geometry. *The
613 American Naturalist*, 174(1), E23–E39. doi:10.1086/599292
- 614 Gauthier, S., Bernier, P., Kuuluvainen, T., Shvidenko, A. Z., & Schepaschenko, D. G. (2015). Boreal forest
615 health and global change. *Science*, 349(6250), 819 LP–822. Retrieved from <http://science.sciencemag.org/>
616 content/349/6250/819.abstract
- 617 Gilman, S. E., Urban, M. C., Tewksbury, J., Gilchrist, G. W., & Holt, R. D. (2010). A framework
618 for community interactions under climate change. *Trends in Ecology & Evolution*, 25(6), 325–331.
619 doi:10.1016/j.tree.2010.03.002
- 620 Goldstein, M. L., Morris, S. A., & Yen, G. G. (2004). Problems with fitting to the power-law distri-
621 bution. *The European Physical Journal B - Condensed Matter and Complex Systems*, 41(2), 255–258.
622 doi:10.1140/epjb/e2004-00316-5
- 623 Haddad, N. M., Brudvig, L. a., Clobert, J., Davies, K. F., Gonzalez, A., Holt, R. D., ... Townshend, J. R.
624 (2015). Habitat fragmentation and its lasting impact on Earth's ecosystems. *Science Advances*, 1(2), 1–9.
625 doi:10.1126/sciadv.1500052
- 626 Hansen, M. C., Potapov, P. V., Moore, R., Hancher, M., Turubanova, S. A., Tyukavina, A., ... Townshend,
627 J. R. G. (2013). High-Resolution Global Maps of 21st-Century Forest Cover Change. *Science*, 342(6160),
628 850–853. doi:10.1126/science.1244693
- 629 Hansen, M., Potapov, P., Margono, B., Stehman, S., Turubanova, S., & Tyukavina, A. (2014). Response
630 to Comment on “High-resolution global maps of 21st-century forest cover change”. *Science*, 344(6187), 981.
631 doi:10.1126/science.1248817
- 632 Hantson, S., Pueyo, S., & Chuvieco, E. (2015). Global fire size distribution is driven by human impact and
633 climate. *Global Ecology and Biogeography*, 24(1), 77–86. doi:10.1111/geb.12246
- 634 Harris, T. E. (1974). Contact interactions on a lattice. *The Annals of Probability*, 2, 969–988.
- 635 Hartigan, J. A., & Hartigan, P. M. (1985). The Dip Test of Unimodality. *The Annals of Statistics*, 13(1),

- 636 70–84. Retrieved from <http://www.jstor.org/stable/2241144>
- 637 Hastings, A., & Wysham, D. B. (2010). Regime shifts in ecological systems can occur with no warning.
- 638 *Ecology Letters*, 13(4), 464–472. doi:10.1111/j.1461-0248.2010.01439.x
- 639 He, F., & Hubbell, S. (2003). Percolation Theory for the Distribution and Abundance of Species. *Physical*
- 640 *Review Letters*, 91(19), 198103. doi:10.1103/PhysRevLett.91.198103
- 641 Heffernan, J. B., Soranno, P. A., Angilletta, M. J., Buckley, L. B., Gruner, D. S., Keitt, T. H., ... Weathers,
- 642 K. C. (2014). Macrosystems ecology: understanding ecological patterns and processes at continental scales.
- 643 *Frontiers in Ecology and the Environment*, 12(1), 5–14. doi:10.1890/130017
- 644 Hinrichsen, H. (2000). Non-equilibrium critical phenomena and phase transitions into absorbing states.
- 645 *Advances in Physics*, 49(7), 815–958. doi:10.1080/00018730050198152
- 646 Hirota, M., Holmgren, M., Nes, E. H. V., & Scheffer, M. (2011). Global Resilience of Tropical Forest and
- 647 Savanna to Critical Transitions. *Science*, 334(6053), 232–235. doi:10.1126/science.1210657
- 648 Irvine, M. A., Bull, J. C., & Keeling, M. J. (2016). Aggregation dynamics explain vegetation patch-size
- 649 distributions. *Theoretical Population Biology*, 108, 70–74. doi:10.1016/j.tpb.2015.12.001
- 650 Keitt, T. H., Urban, D. L., & Milne, B. T. (1997). Detecting critical scales in fragmented landscapes.
- 651 *Conservation Ecology*, 1(1), 4. Retrieved from <http://www.ecologyandsociety.org/vol1/iss1/art4/>
- 652 Kéfi, S., Guttal, V., Brock, W. A., Carpenter, S. R., Ellison, A. M., Livina, V. N., ... Dakos, V. (2014).
- 653 Early Warning Signals of Ecological Transitions: Methods for Spatial Patterns. *PLoS ONE*, 9(3), e92097.
- 654 doi:10.1371/journal.pone.0092097
- 655 Kéfi, S., Rietkerk, M., Alados, C. L., Pueyo, Y., Papanastasis, V. P., ElAich, A., & Ruiter, P. C. de.
- 656 (2007). Spatial vegetation patterns and imminent desertification in Mediterranean arid ecosystems. *Nature*,
- 657 449(7159), 213–217. doi:10.1038/nature06111
- 658 Kitzberger, T., Aráoz, E., Gowda, J. H., Mermoz, M., & Morales, J. M. (2012). Decreases in Fire Spread
- 659 Probability with Forest Age Promotes Alternative Community States, Reduced Resilience to Climate Vari-
- 660 ability and Large Fire Regime Shifts. *Ecosystems*, 15(1), 97–112. doi:10.1007/s10021-011-9494-y
- 661 Koenker, R. (2016). quantreg: Quantile Regression. Retrieved from <http://cran.r-project.org/package=quantreg>
- 663 Lasco, R. D., Pulhin, F. B., Cruz, R. V. O., Pulhin, J. M., Roy, S. S. N., & Sanchez, P. A. J. (2008). Forest
- 664 responses to changing rainfall in the Philippines. In N. Leary, C. Conde, & J. Kulkarni (Eds.), *Climate*

- 665 change and vulnerability (pp. 49–66). London: Earthscan. Retrieved from <http://gen.lib.rus.ec/book/index.php?md5=AD313B13E05C9D61A9EC1EE2E73A91FB>
- 666
- 667 Leibold, M. A., & Norberg, J. (2004). Biodiversity in metacommunities: Plankton as complex adaptive
668 systems? *Limnology and Oceanography*, 49(4, part 2), 1278–1289. doi:10.4319/lo.2004.49.4_part_2.1278
- 669 Lenton, T. M., & Williams, H. T. P. (2013). On the origin of planetary-scale tipping points. *Trends in
670 Ecology & Evolution*, 28(7), 380–382. doi:10.1016/j.tree.2013.06.001
- 671 Lenton, T. M., Held, H., Kriegler, E., Hall, J. W., Lucht, W., Rahmstorf, S., & Schellnhuber, H. J. (2008).
672 Tipping elements in the Earth's climate system. *Proceedings of the National Academy of Sciences*, 105(6),
673 1786–1793. doi:10.1073/pnas.0705414105
- 674 Limpert, E., Stahel, W. A., & Abbt, M. (2001). Log-normal Distributions across the Sciences: Keys and
675 CluesOn the charms of statistics, and how mechanical models resembling gambling machines offer a link to
676 a handy way to characterize log-normal distributions, which can provide deeper insight into var. *BioScience*,
677 51(5), 341–352. Retrieved from [http://dx.doi.org/10.1641/0006-3568\(2001\)051\[0341:LNDATS\]2.0.CO](http://dx.doi.org/10.1641/0006-3568(2001)051[0341:LNDATS]2.0.CO)
- 678 Loehle, C., Li, B.-L., & Sundell, R. C. (1996). Forest spread and phase transitions at forest-prairie ecotones
679 in Kansas, U.S.A. *Landscape Ecology*, 11(4), 225–235.
- 680 Malhi, Y., Gardner, T. A., Goldsmith, G. R., Silman, M. R., & Zelazowski, P. (2014). Tropical Forests in
681 the Anthropocene. *Annual Review of Environment and Resources*, 39(1), 125–159. doi:10.1146/annurev-
682 environ-030713-155141
- 683 Manor, A., & Shnerb, N. M. (2008). Origin of pareto-like spatial distributions in ecosystems. *Physical
684 Review Letters*, 101(26), 268104. doi:10.1103/PhysRevLett.101.268104
- 685 Martensen, A. C., Ribeiro, M. C., Banks-Leite, C., Prado, P. I., & Metzger, J. P. (2012). Associations
686 of Forest Cover, Fragment Area, and Connectivity with Neotropical Understory Bird Species Richness and
687 Abundance. *Conservation Biology*, 26(6), 1100–1111. doi:10.1111/j.1523-1739.2012.01940.x
- 688 McKenzie, D., & Kennedy, M. C. (2012). Power laws reveal phase transitions in landscape con-
689 trols of fire regimes. *Nat Commun*, 3, 726. Retrieved from <http://dx.doi.org/10.1038/ncomms1731>
690 http://www.nature.com/ncomms/journal/v3/n3/supplinfo/ncomms1731{_\}S1.html
- 691 Mitchell, M. G. E., Suarez-Castro, A. F., Martinez-Harms, M., Maron, M., McAlpine, C., Gaston, K. J., ...
692 Rhodes, J. R. (2015). Reframing landscape fragmentation's effects on ecosystem services. *Trends in Ecology*

- 693 *& Evolution*, 30(4), 190–198. doi:10.1016/j.tree.2015.01.011
- 694 Naito, A. T., & Cairns, D. M. (2015). Patterns of shrub expansion in Alaskan arctic river corridors suggest
695 phase transition. *Ecology and Evolution*, 5(1), 87–101. doi:10.1002/ece3.1341
- 696 Newman, M. E. J. (2005). Power laws, Pareto distributions and Zipf's law. *Contemporary Physics*, 46(5),
697 323–351. doi:10.1080/00107510500052444
- 698 Oborny, B., Meszéna, G., & Szabó, G. (2005). Dynamics of Populations on the Verge of Extinction. *Oikos*,
699 109(2), 291–296. Retrieved from <http://www.jstor.org/stable/3548746>
- 700 Oborny, B., Szabó, G., & Meszéna, G. (2007). Survival of species in patchy landscapes: percolation in
701 space and time. In *Scaling biodiversity* (pp. 409–440). Cambridge University Press. Retrieved from <http://dx.doi.org/10.1017/CBO9780511814938.022>
- 703 Ochoa-Quintero, J. M., Gardner, T. A., Rosa, I., de Barros Ferraz, S. F., & Sutherland, W. J. (2015).
704 Thresholds of species loss in Amazonian deforestation frontier landscapes. *Conservation Biology*, 29(2),
705 440–451. doi:10.1111/cobi.12446
- 706 Ódor, G. (2004). Universality classes in nonequilibrium lattice systems. *Reviews of Modern Physics*, 76(3
707 I), 663–724. doi:10.1103/RevModPhys.76.663
- 708 Pardini, R., Bueno, A. de A., Gardner, T. A., Prado, P. I., & Metzger, J. P. (2010). Beyond the Fragmen-
709 tation Threshold Hypothesis: Regime Shifts in Biodiversity Across Fragmented Landscapes. *PLoS ONE*,
710 5(10), e13666. doi:10.1371/journal.pone.0013666
- 711 Potapov, P., Hansen, M. C., Stehman, S. V., Loveland, T. R., & Pittman, K. (2008). Combining MODIS
712 and Landsat imagery to estimate and map boreal forest cover loss. *Remote Sensing of Environment*, 112(9),
713 3708–3719. doi:<https://doi.org/10.1016/j.rse.2008.05.006>
- 714 Potapov, P., Yaroshenko, A., Turubanova, S., Dubinin, M., Laestadius, L., Thies, C., ... Zhuravleva, I. (2008).
715 Mapping the world's intact forest landscapes by remote sensing. *Ecology and Society*, 13(2).
- 716 Prishchepov, A. V., Müller, D., Dubinin, M., Baumann, M., & Radeloff, V. C. (2013). Determinants
717 of agricultural land abandonment in post-Soviet European Russia. *Land Use Policy*, 30(1), 873–884.
718 doi:<https://doi.org/10.1016/j.landusepol.2012.06.011>
- 719 Pueyo, S., de Alencastro Graça, P. M. L., Barbosa, R. I., Cots, R., Cardona, E., & Fearnside, P. M. (2010).
720 Testing for criticality in ecosystem dynamics: the case of Amazonian rainforest and savanna fire. *Ecology*

- 721 *Letters*, 13(7), 793–802. doi:10.1111/j.1461-0248.2010.01497.x
- 722 R Core Team. (2015). R: A Language and Environment for Statistical Computing. Vienna, Austria: R
723 Foundation for Statistical Computing. Retrieved from <http://www.r-project.org/>
- 724 Reyer, C. P. O., Rammig, A., Brouwers, N., & Langerwisch, F. (2015). Forest resilience, tipping points and
725 global change processes. *Journal of Ecology*, 103(1), 1–4. doi:10.1111/1365-2745.12342
- 726 Rockstrom, J., Steffen, W., Noone, K., Persson, A., Chapin, F. S., Lambin, E. F., ... Foley, J. A. (2009). A
727 safe operating space for humanity. *Nature*, 461(7263), 472–475. Retrieved from <http://dx.doi.org/10.1038/461472a>
- 729 Rooij, M. M. J. W. van, Nash, B., Rajaraman, S., & Holden, J. G. (2013). A Fractal Approach to Dynamic
730 Inference and Distribution Analysis. *Frontiers in Physiology*, 4(1). doi:10.3389/fphys.2013.00001
- 731 Saravia, L. A., & Momo, F. R. (2017). Biodiversity collapse and early warning indicators in
732 a spatial phase transition between neutral and niche communities. *PeerJ PrePrints*, 5, e1589v4.
733 doi:10.7287/peerj.preprints.1589v3
- 734 Scanlon, T. M., Caylor, K. K., Levin, S. A., & Rodriguez-iturbe, I. (2007). Positive feedbacks promote
735 power-law clustering of Kalahari vegetation. *Nature*, 449(September), 209–212. doi:10.1038/nature06060
- 736 Scheffer, M., Bascompte, J., Brock, W. A., Brovkin, V., Carpenter, S. R., Dakos, V., ... Sugihara, G. (2009).
737 Early-warning signals for critical transitions. *Nature*, 461(7260), 53–59. doi:10.1038/nature08227
- 738 Scheffer, M., Walker, B., Carpenter, S., Foley, J. a, Folke, C., & Walker, B. (2001). Catastrophic shifts in
739 ecosystems. *Nature*, 413(6856), 591–596. doi:10.1038/35098000
- 740 Seidler, T. G., & Plotkin, J. B. (2006). Seed Dispersal and Spatial Pattern in Tropical Trees. *PLoS Biology*,
741 4(11), e344. doi:10.1371/journal.pbio.0040344
- 742 Sexton, J. O., Noojipady, P., Song, X.-P., Feng, M., Song, D.-X., Kim, D.-H., ... Townshend, J. R.
743 (2015). Conservation policy and the measurement of forests. *Nature Climate Change*, 6(2), 192–196.
744 doi:10.1038/nclimate2816
- 745 Sexton, J. O., Song, X.-P., Feng, M., Noojipady, P., Anand, A., Huang, C., ... Townshend, J. R. (2013).
746 Global, 30-m resolution continuous fields of tree cover: Landsat-based rescaling of MODIS vegetation con-
747 tinuous fields with lidar-based estimates of error. *International Journal of Digital Earth*, 6(5), 427–448.
748 doi:10.1080/17538947.2013.786146
- 749 Solé, R. V. (2011). *Phase Transitions* (p. 223). Princeton University Press. Retrieved from <https://books.google.com/books?id=KUWzDwAAQBAJ&pg=PA223&lpg=PA223&dq=phase+transitions+R.+V.+S%C3%B3l%C3%A9&hl=en&sa=X&ved=0ahUKEwjL4IuGxMfAahUKEwip0dCqBbUAQ6wE&qid=1480330700811&sr=1>

- 750 google.com.ar/books?id=8RcLuv-Ll2kC
- 751 Solé, R. V., & Bascompte, J. (2006). *Self-organization in complex ecosystems* (p. 373). New Jersey, USA.:
752 Princeton University Press. Retrieved from <http://books.google.com.ar/books?id=v4gpGH6Gv68C>
- 753 Solé, R. V., Alonso, D., & Mckane, A. (2002). Self-organized instability in complex ecosystems. *Philosophical Transactions of the Royal Society of London. Series B, Biological Sciences*, 357(May), 667–681.
754
755 doi:10.1098/rstb.2001.0992
- 756 Solé, R. V., Alonso, D., & Saldaña, J. (2004). Habitat fragmentation and biodiversity collapse in neutral
757 communities. *Ecological Complexity*, 1(1), 65–75. doi:10.1016/j.ecocom.2003.12.003
- 758 Solé, R. V., Bartumeus, F., & Gamarra, J. G. P. (2005). Gap percolation in rainforests. *Oikos*, 110(1),
759 177–185. doi:10.1111/j.0030-1299.2005.13843.x
- 760 Staal, A., Dekker, S. C., Xu, C., & Nes, E. H. van. (2016). Bistability, Spatial Interaction, and the
761 Distribution of Tropical Forests and Savannas. *Ecosystems*, 19(6), 1080–1091. doi:10.1007/s10021-016-0011-
762 1
- 763 Stauffer, D., & Aharony, A. (1994). *Introduction To Percolation Theory* (p. 179). London: Taylor & Francis.
- 764 Vasilakopoulos, P., & Marshall, C. T. (2015). Resilience and tipping points of an exploited fish population
765 over six decades. *Global Change Biology*, 21(5), 1834–1847. doi:10.1111/gcb.12845
- 766 Verbesselt, J., Umlauf, N., Hirota, M., Holmgren, M., Van Nes, E. H., Herold, M., ... Scheffer, M. (2016). Re-
767 motely sensed resilience of tropical forests. *Nature Climate Change*, 1(September). doi:10.1038/nclimate3108
- 768 Villa Martín, P., Bonachela, J. A., & Muñoz, M. A. (2014). Quenched disorder forbids discontinuous
769 transitions in nonequilibrium low-dimensional systems. *Physical Review E*, 89(1), 12145. Retrieved from
770 <https://link.aps.org/doi/10.1103/PhysRevE.89.012145>
- 771 Villa Martín, P., Bonachela, J. A., Levin, S. A., & Muñoz, M. A. (2015). Eluding catastrophic shifts.
772 *Proceedings of the National Academy of Sciences*, 112(15), E1828–E1836. doi:10.1073/pnas.1414708112
- 773 Viña, A., McConnell, W. J., Yang, H., Xu, Z., & Liu, J. (2016). Effects of conservation policy on China's
774 forest recovery. *Science Advances*, 2(3), e1500965. Retrieved from <http://advances.sciencemag.org/content/2/3/e1500965.abstract>
- 776 Vuong, Q. H. (1989). Likelihood Ratio Tests for Model Selection and Non-Nested Hypotheses. *Econometrica*,
777 57(2), 307–333. doi:10.2307/1912557
- 778 Weerman, E. J., Van Belzen, J., Rietkerk, M., Temmerman, S., Kéfi, S., Herman, P. M. J., & Koppell, J. V.

- 779 de. (2012). Changes in diatom patch-size distribution and degradation in a spatially self-organized intertidal
780 mudflat ecosystem. *Ecology*, 93(3), 608–618. doi:10.1890/11-0625.1
- 781 Weissmann, H., & Shnerb, N. M. (2016). Predicting catastrophic shifts. *Journal of Theoretical Biology*, 397,
782 128–134. doi:10.1016/j.jtbi.2016.02.033
- 783 Wuyts, B., Champneys, A. R., & House, J. I. (2017). Amazonian forest-savanna bistability and human
784 impact. *Nature Communications*, 8(May), 15519. doi:10.1038/ncomms15519
- 785 Xu, C., Hantson, S., Holmgren, M., Nes, E. H. van, Staal, A., & Scheffer, M. (2016). Remotely sensed
786 canopy height reveals three pantropical ecosystem states. *Ecology*, 97(9), 2518–2521. doi:10.1002/ecy.1470
- 787 Zhang, J. Y., Wang, Y., Zhao, X., Xie, G., & Zhang, T. (2005). Grassland recovery by protection from
788 grazing in a semi-arid sandy region of northern China. *New Zealand Journal of Agricultural Research*, 48(2),
789 277–284. doi:10.1080/00288233.2005.9513657
- 790 Zinck, R. D., & Grimm, V. (2009). Unifying wildfire models from ecology and statistical physics. *The
791 American Naturalist*, 174(5), E170–85. doi:10.1086/605959